J Sol-Gel Sci Technol (2017) 81:177–184
DOI 10.1007/s10971-016-4186-x

ORIGINAL PAPER: FUNDAMENTALS OF SOL-GEL AND HYBRID MATERIALS PROCESSING

Improvement in electronic and magnetic transport of $La_{0.67}Ca_{0.33}MnO_3$ manganites by optimizing sintering temperature

Fei Jin[1] · Hui Zhang[1] · Xiaohui Chen[1] · Xiang Liu[1] · Qingming Chen[1]

Received: 25 June 2016 / Accepted: 12 August 2016 / Published online: 13 September 2016

Abstract $La_{0.67}Ca_{0.33}MnO_3$ samples with high temperature coefficient of resistance have been synthesized by sol-gel method using methyl alcohol as solvent. Nitrates of La, Ca and Mn were heated with a controlled amount of methyl alcohol to get a dry powder which on suitable heat treatment gave high grade $La_{0.67}Ca_{0.33}MnO_3$ powder/pellets. The samples were sintered in the temperature varied from 1000 °C to 1550 °C. The effects of sintering temperature (T_s) on phase purity, microstructure, morphology, electrical and magnetic transport properties have been investigated. The results confirm that elevated sintering temperature at sintering processing accelerates the growth of the specimen grains, influence microstructure and improves chemical homogeneity, which leads to the increased lattice distortion and thus contributes to the enhancement of magneto-resistance. The reduction of the grain boundaries contributes to the reduction of resistivity and the enhancement of the coefficient of resistance. The increase of the oxygen vacancy induced by the increase of T_s will lead to monotonous decrease of the metal-insulator transition temperature (T_p), the peak of temperature for the maximum temperature coefficient of resistance (T_k) and for the peak of maximum magneto-resistance (T_m).

Graphical Abstract

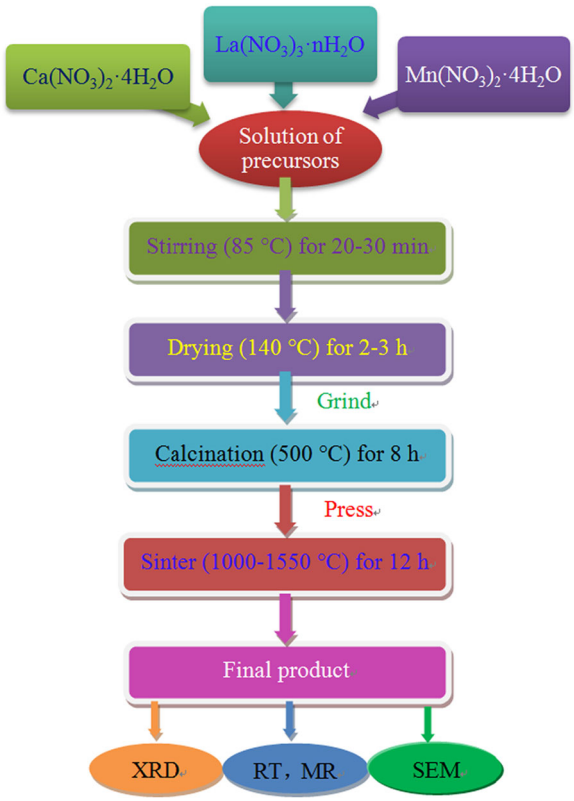

Keywords Sol-gel method · Electronic · Magnetic · Sintering temperature

1 Introduction

The rare earth-doped perovskite manganite, $La_{1-x}AE_xMnO_3$ (AE=Ca, Ba, Sr, etc.)has received considerable attention in the past decades, because of its unusual colossal magneto-

✉ Qingming Chen
qmchen99@163.com

[1] Faculty of Materials Science and Engineering, Kunming University of Science and Technology, Kunming 650093, China

resistance (CMR) effects and potential applications in magnetic switch, infrared (IR) detector and magnetic sensor [1–4]. Among the rare earth-doped manganite family, samples dopedwith divalent cation Ca exhibit the optimal and enhanced double-exchange effect, which brings more superior and outstanding physical properties in comparison with other doping contents of CMR materials. At Ca concentration of 0.17–0.5, whereCMR effect is observed, the material shows a paramagnetic insulation to ferromagneticmetal transition with the change inthe ambient temperature [5]. It has been known that CMR effect depends on the Mn^{4+}/Mn^{3+} ratio, which can be adjusted by doping and oxygen content [6, 7]. The Mn^{3+}/Mn^{4+} ratio is one of the parameters that can effectively control different interactions such as double exchange, super-exchange and Coulomb interaction among Mn ions. The variations in theMn–O–Mn bond length and bond angle, change the electron hopping and carrier localization and therefore determine the electronic and magnetic transport properties of thematerials [8].

Sintering is a typical treatment to modify the particle behavior, and the sintering temperature (T_s) is frequently employed as a key parameter to control the quality of ceramic powders [9–11], sinceT_s plays a vital role in the evolution of microstructure and morphologies for the powders. In addition, improving the preparation condition and doping different elements can also modify the electronic and magnetic transport properties due to their influence on microstructure, crystallization and homogeneity. It is possible for CMR materials to obtain the sharpness of the temperature coefficient of resistance (TCR) and metal-insulator transition temperature (T_p) nearly room temperature [12].

There are several synthesis methods, including the conventionalsolid-state reaction, co-precipitation, reactive milling, spray-drying, sol-gel method, etc. have been developed for the synthesisdoped manganites [13–17]. Among these methods, the sol-gel method is outstanding from the point of process simplicity, excellent reproducibility and high pure-phase, and can produce nanoscale powders with better chemical uniformity and desired stoichiometry.The reagents are mixed at molecular level, which accelerates thereaction rate, reduces the synthesis temperature and has betteruniformity. Unlike other chemical routes, there are no filtration and washing of the precipitate and hence the composition and purity can be controlled very easily. But there are some problems to await to settle in the conventional sol-gel producecraftwork, for instance, thecomplexcraftwork, sophisticatedequipment, lowyield, costly reagents and long processing time, etc.The method described here is quite simple and quick, still the quality of the product is very good as reflected by the high surface area and purity of the powder and the high bulk density and high TCR of the pellet.

In the present work, a simple and effective method of "methyl alcohol route", developed by us to be promising to fabricate high purity and homogeneity of perovskite manganites because of its simplicity andtime saving aspect, ispresented. Further, we investigated the possibility of modifying the microstructure, pores, grain boundaries and grain sizes by changing T_s, and furthermore to improve the electronic and magnetic transport properties of LCMO ceramics.

2 Materials and methods

The $La_{0.67}Ca_{0.33}MnO_3$ (LCMO) powders were synthesized by sol-gel method. First of all, the starting compounds i.e., $La(NO_3)_3{\cdot}nH_2O$, $Ca(NO_3)_2{\cdot}4H_2O$, $Mn(NO_3)_2{\cdot}4H_2O$ were dissolved in methyl alcohol with a molar ratio of 2:1:3 to form a solution, the molar ratio of the metal atom and citric acid was 1:2. Ethylene glycol was added as a cross-linking agent. The mixture was continuously stirred and heated at 85 °C for several minutes in the magnetic stirring apparatus. Then, the gel was dried in an oven at 140 °C for 2 h and ground in an agate mortar for 15 min to obtain the precursor powders.The powders were calcined at 500 °C for 8 h to achieve single phase LCMO. Finally, the resulting powders were ground again and pressed into pellets with diameter (a) of 20 mm, and the pellets were sintered from 1000 °C to 1550 °C in the air for 8 h to get bulk polycrystalline ceramic targets. The steps involved in the present method are shown in the schematic Fig. 1.

The crystal structure of the samples were characterized by X-ray diffraction (XRD) using a D8 Focus diffractometer (Bruker) with Cu K_α radiation ($\lambda = 1.5406$ Å) in the 2θ range from 20 ° to 80 °. The temperature dependence of resistivity and magneto-resistivity (ρ-T) of the bulk was measured in the temperature range from 150 K to 300 K under 0–1 T field by using a four-probe magneto-resistance system. The size and the shapes of particles were directly observed by scanning electron microscope (SEM) using a VEGA3 TESCAN instrument.

3 Results and discussion

To study the effect of sintering temperature on the electronic and magnetic transport properties, $La_{0.67}Ca_{0.33}MnO_3$ samples were sintered at eight different temperatures from 1000 °C to 1550 °C.

The XRD patterns of LCMO ceramics samples sintered at different temperatures are shown in Fig. 2(a). It can be seen from Fig. 2(a) that all the samples have the orthorhombic perovskite structure of Pnma space group and without any detectable secondary phase. All measured

diffraction patterns matches those of the $La_{0.67}Ca_{0.33}MnO_3$ (JCPDS card no: 49-0616) perfectly. Figure 2(b) shows the enlarged strongest peak (121) with different T_s. The diffraction peak (121) shifts to a lower diffraction angle as the T_s increases, which implies the increase of the lattice parameter.Using XRD data Fig. 2(a), the lattice parameters of LCMO samples were calculated by using MDI Jade6.5 software. Table 1 presents the lattice constant data of all samples. The latticeparameter increases slightly as the elevation of sintering temperature for the specimens of LCMO. This can be attributed to the increasein Mn–O bond length[18]. The same result has been reported in $La_{0.7}Ca_{0.3}MnO_3$ [19].

Sintering process is adynamicprocesswithdensification and grain growth simultaneously, but the densification and grain growth are competing processes. The densification of nanoparticles is strongly affected by agglomeration of particles, pores and other processing variables [20].The grain

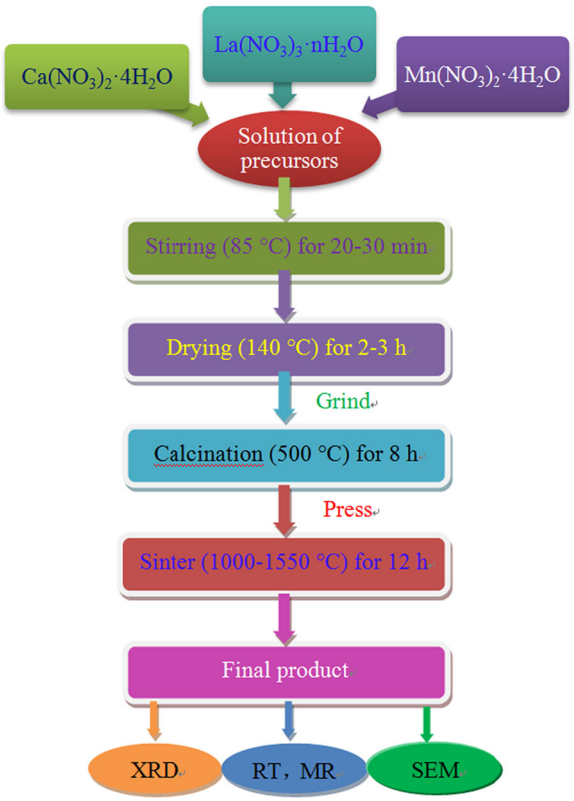

Fig. 1 Flow diagram of Sol-gel method used to synthesize high grade LCMO polycrystalline ceramics

Table 1 Values of T_p, lattice parameters (a), T_k, T_m, MR, TCR, and resistivity of LCMO samples

T_s(°C)	T_p (K)		a(Å)	T_k(K)	T_m(K)	MR%	TCR ($\%K^{-1}$)	ρ(Ω·cm)
	0T	1T						
1000	274.6	277.9	5.451	268.9	272.5	20.2	5.2	0.07382
1100	269.8	279.5	5.453	267.7	268	34.4	9.8	0.03863
1250	269.5	278.8	5.459	266.0	267.1	41.1	15.6	0.02883
1350	266.4	276.6	5.473	263.8	264.1	45.7	22.6	0.01832
1400	265.5	277.3	5.473	261.7	262.9	50.3	24.9	0.01712
1450	264.5	276.5	5.482	259.9	259.9	57.5	40.3	0.01604
1500	264.0	277.0	5.483	259.3	259.9	61.6	30.7	0.01817
1550	264.5	277.5	5.486	257.6	259.3	66.6	28.9	0.01939

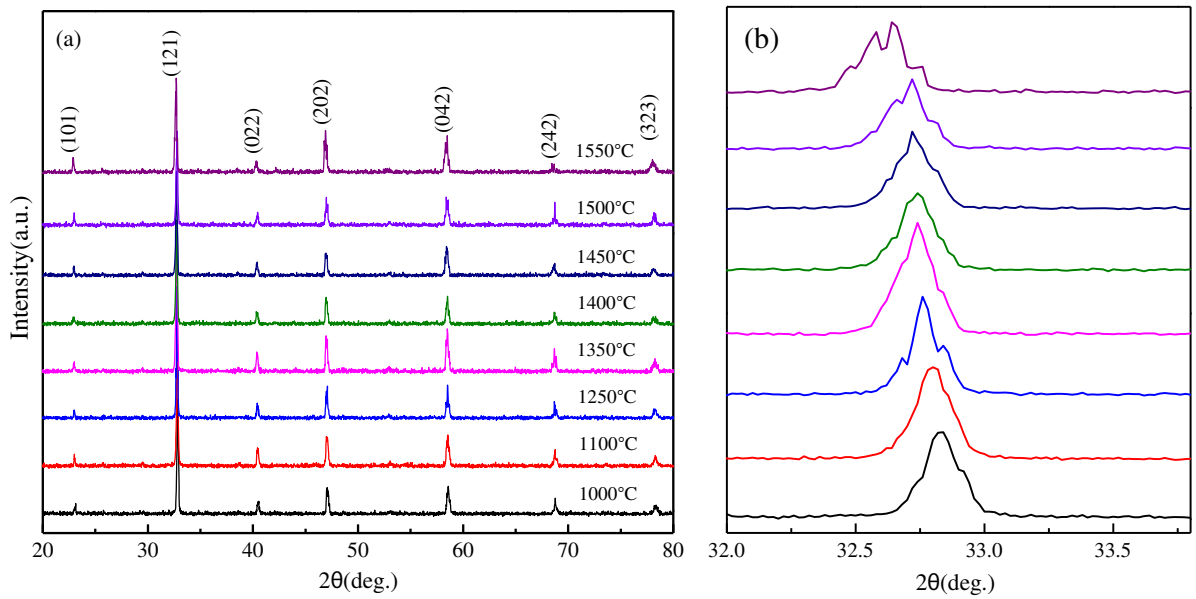

Fig. 2 **a** XRD patterns of $La_{0.67}Ca_{0.33}MnO_3$ samples sintered at different temperatures and **b** the enlarged strongest peak (121)

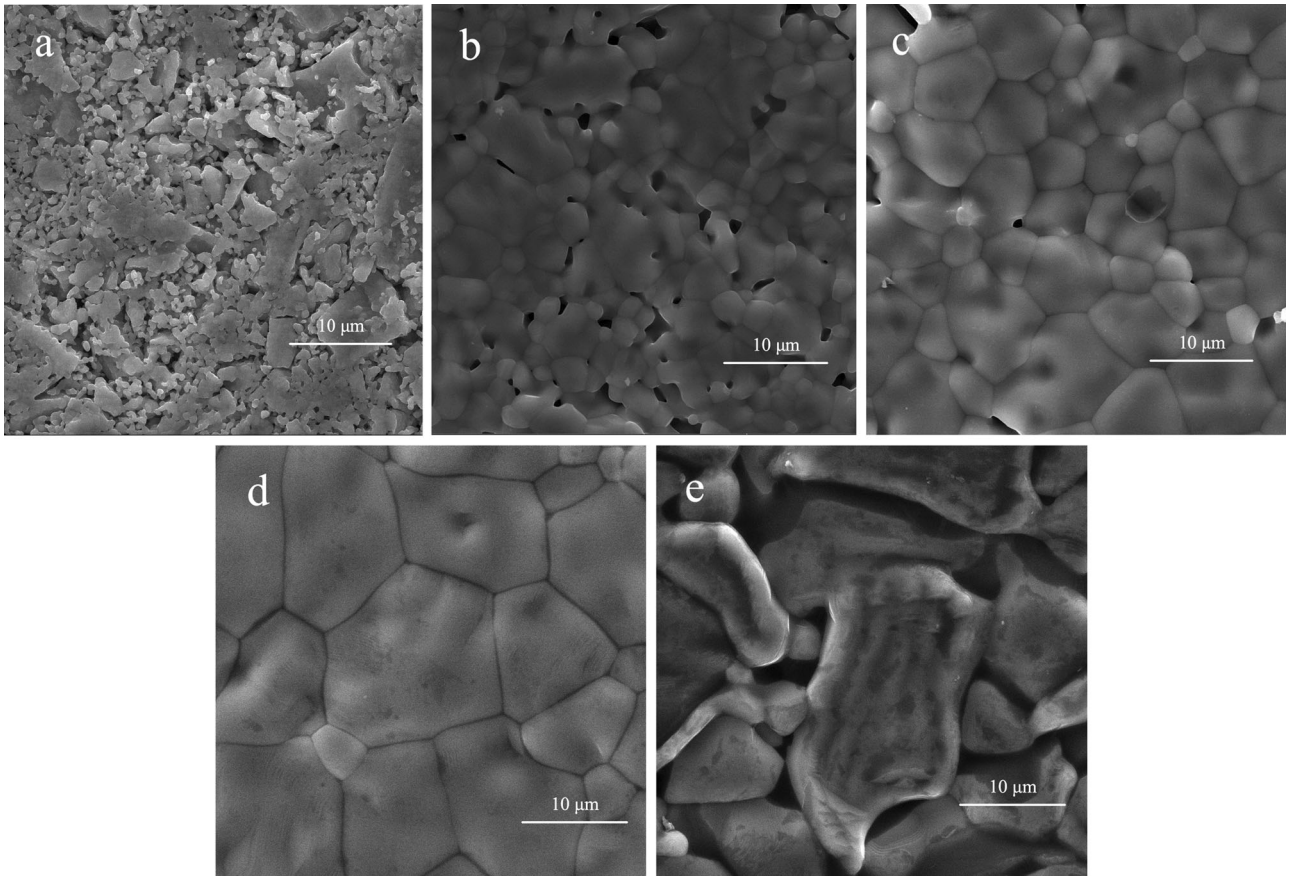

Fig. 3 SEM micrographs of LCMO ceramics sintered at **a** 1000 °C, **b** 1250 °C, **c** 1350°C, **d** 1450 °C, **e** 1550 °C

growth in the calcination process, removes the original stress and makes the grain structure quite stable. The calcined powders have higher surface energy, and the higher T_s promote the growth and densification of grain sizes.

Special attention should be paid to the overall microstructural evolution owing to the temperature variation. The general microstructures of all the samples are presented in Fig. 3, at the same magnification of 10 μm for intercomparison. It can be measured from the SEM images that the average grain sizes of LCMO with Ts = 1000, 1250, 1350, 1450, 1550 °C are 0.5, 4.8, 8.6, 18.2 and 21.2 μm, respectively, which increase monotonically with the increase in sintering temperature. When the grain size increases, the grain becomes moredensely packed resulting in narrowing of the grainboundary regions. It benefits the conduction of electric carriers, which is responsible for the improvement of the conductivity. Figure 3(a) reveals an agglomerated particle with cage like morphology. There are no visible grains and grain boundaries in the sample.This is attributed to the lower T_s. A porous microstructure with small grain size is observed in the sample sintered at 1250 °C. The increase of T_s significantly promotes the grain growth and microstructural densification. The grain size reaches the maximum value at 1450 °C and becomes uniform, which indicates that the homogeneity and well crystallization of the sample. However, the sample is oversintered which led to grain growth inhomogeneous and the number of pore increased, when the temperature exceeded about 1550 °C.

The resistivity, studied throughout the temperature range, decreases with increasing sintering temperature for boththe systems studied.The plots of resistivity (ρ) as a function of temperature for LCMO ceramics, are shown in Fig. 4. All curves clearly exhibit that sharp metal-insulator transition is happening nearby T_p (values of T_p are listed in Table 1). It is observed that with elevating T_s from 1000 to 1550 °C, the value of T_p at zero-field, the peak of temperature for the maximum temperature coefficient of resistance (T_k) and the peak of maximum magneto-resistance (T_m) monotonically shift towards lower temperature region from 276.4 to 264.0 K, 268.9 to 257.6 K and 272.5 to 259.3 K, respectively. There is a mismatch with that reported in literature [21]. We now suggest that the reason for the observed decrease of T_p with increasing T_s may be the enhanced oxygen deficiency with increasing T_s [22]. According to the double-exchange theory, the conduction in manganites achieves via hopping of e_g electrons between Mn^{3+} and Mn^{4+} with the help of intermediate oxygen ions. The occurrence of oxygen

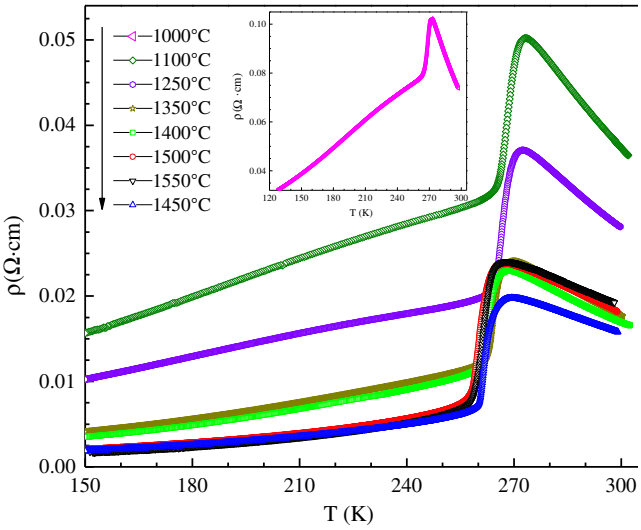

Fig. 4 Resistivity-temperature plots for different T_s values obtained at zero-field

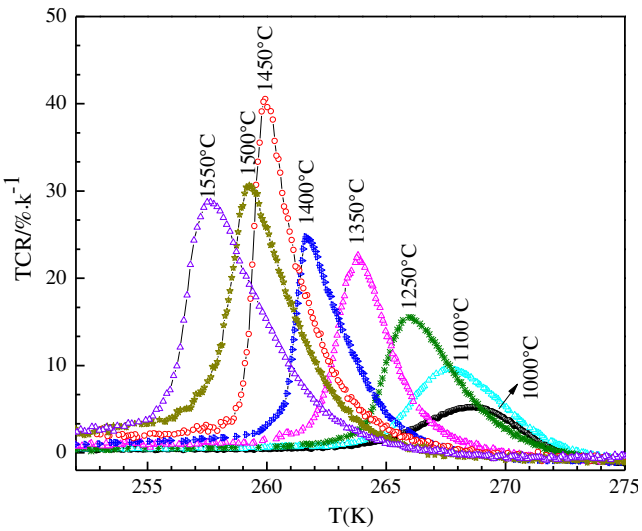

Fig. 5 TCR versus temperature curves of $La_{0.67}Ca_{0.33}MnO_3$ samples with different sintering temperatures

vacancies would break the hopping bridge for e_g electrons, resulting in decrease of the density of charge carriers, which further results in decrease of T_p and broadening of the resistivity peak [23].

We all know that TCR is one of the important parameters to improve the sensitivity of uncooled infrared microbolometer. In this study, Fig. 5 shows the temperature dependence of TCR, from Fig. 4. It shows the peak of temperature for the maximum TCR (T_k) continuously shifting to lower temperatures, as T_s increases, and the values of TCR decrease at first and then increase in Fig. 7(b). With the T_s of 1450 °C, the TCR value reached its maximum of 40.2 %·K^{-1}, almost eight times higher than that of 1000 °C. This is attributed to the increase in average grain size with increasing T_s, which results in the decreased grain boundary density leading to weakness in the scattering of charge carriers at the grain boundary. There is a weakened double exchange effect and increased residual resistivity in LCMO bulk sintered above 1450 °C, implying a considerable increase in the amount of pores and resulting in creating spin polarized tunneling effect, leading to the attenuation of TCR.

The variation of resistivity (ρ) with temperature from 150 to 300 K of all the samples measured under zero and 1T magnetic field are shown in Fig. 6. Temperature dependence of magneto-resistance (MR) of LCMO ceramics are shown in the inset of Fig. 6. MR is defined as MR % = (ρ(0,T)-ρ(H,T)/ρ(0,T)) × 100 %, where ρ(0,T) and ρ(H,T) are the resistivity in zero and 1T field, respectively. It is observed that the application of magnetic field induces delocalization of charge carriers, which in turn might suppress the electrical resistivity and lead to shiftof the T_p towards higher temperatures, thereby resulting in increase of metallic phase fraction. This is attributed to the induced magnetic ordering of the localized t_{2g} spins and production of more free charge carriers on application of magnetic field [24]. However, according to Table 1, the value of T_p in the LCMO ceramics are little changed in applied magnetic fields (1T), this may be the magnetization increases with the decrease of the grain boundary effect. The values of the resistivity of all the samples are comparative or even smaller than that of single crystals prepared by Markovich et al. [25], confirming the good quality of our samples. Figure. 7(a) shows a linear relationship between the T_s and the MR.

Clearly, optimized elevating T_s improves the electrical, magneto-transport properties of LCMO significantly, which may be due to the enhancement of grain growth that improves the connectivity between the grains and reduces the existence of pores and voids, and thus enhances the electrical properties.

4 Conclusions

LCMO polycrystalline samples have been synthesized by sol-gel method. The “methyl alcohol route” developed by us for the preparation of LCMO powder is outstanding from the point of process simplicity, low cost and short processing time. The bulks sintered at different temperatures and the correlation between structure, morphologies, electrical and magneto-transport properties motivated by various $T_s$have been investigated. The T_s plays a vital role in the evolution of microstructure and morphologies. The

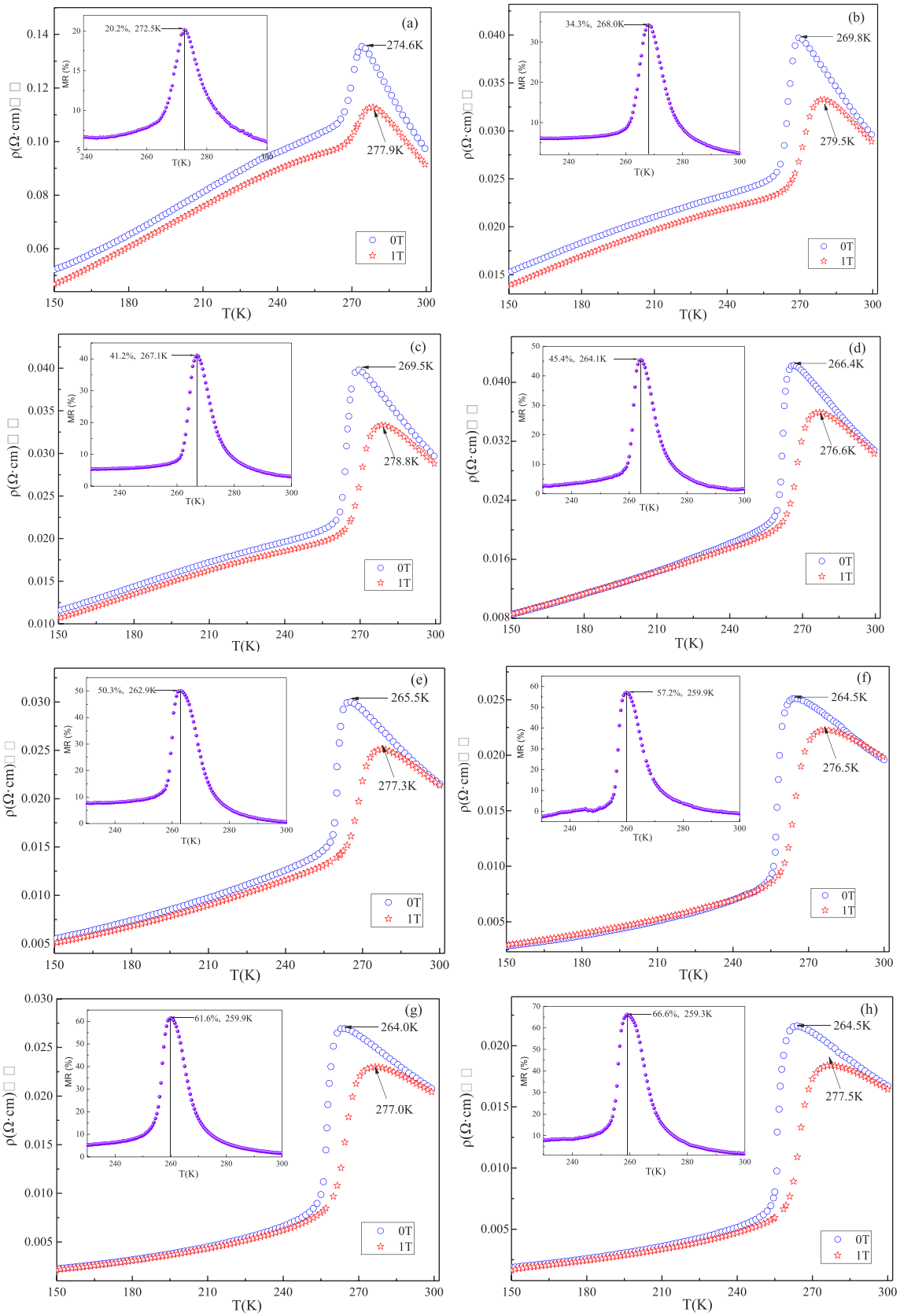

Fig. 6 Resistivity-temperature variation with and without magnetic field of LCMO ceramics; the inset shows the MR % ratio versus temperature at 1 T

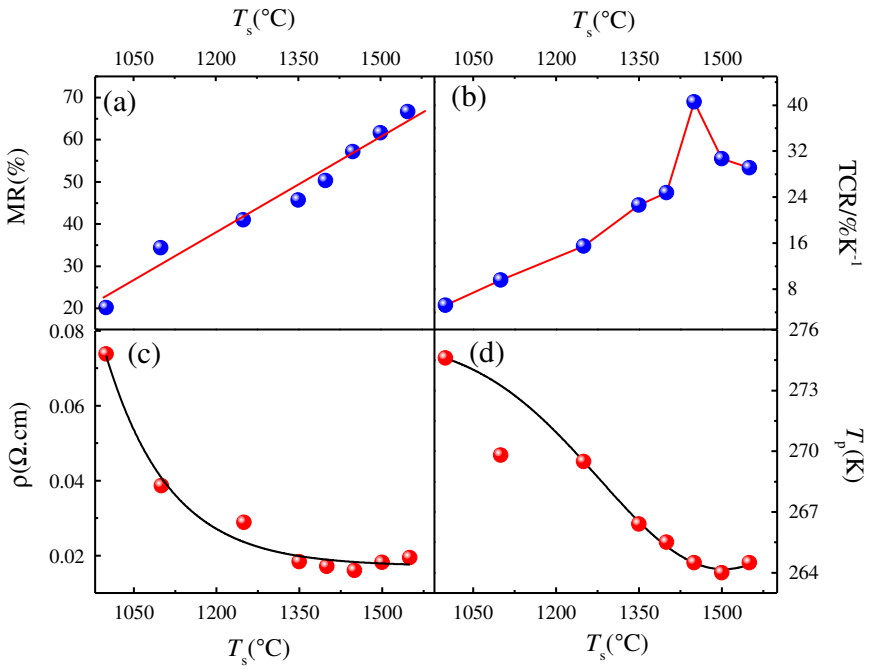

Fig. 7 Dependence of **a** MR, **b** TCR, **c** ρ and **d** T_p of the LCMO ceramics with the T_s

microstructure morphology analysis indicates that it can accelerate the growth of the grains and improve homogeneity by elevated T_s, which contributes to the increase of MR and sharp metal-insulator transition. Besides, the decrease in the ratio of Mn^{4+}/Mn^{3+} due to the increase in oxygen vacancy is the main reason for the significant reduction in the T_p of LCMO ceramics from 274.6 to 264 K.

Acknowledgments This work was supported by the National Natural Science Foundation of China (Grant No. 11564021).

Compliance with ethical standards

Conflict of interest The authors declare that they have no conflict of interests.

References

1 Helmoh RV, Wecker J, Holzapfel B et a1. (1993) Giant negative magnetoresistance in perovskitelike $La_{2/3}Ba_{l/3}MnO_x$ ferromagnetic films. Phys Rev Lett 71:2331
2 Dagotto E, Hotta T, Moreo A (2001) Colossal magnetoresistant materials: the key role of phase separation. Phys Rep 344:1–153
3 Huang YH, Yan CH, Luo F et al. (2002) Large enhancement in room-temperature magnetoresistance and dramatic decrease in resistivity in $La_{0.7}Ca_{0.3}MnO_3$-Ag composites. Appl Phys Lett 81:76–78
4 Awana VPS, Tripathi R, Balamurugan S et al. (2006) Magneto-transport of high TCR (temperature coefficient of resistance) $La_{2/3}Ca_{1/3}MnO_3$:Ag polycrystalline composites. Solid State Commun 120:410–415
5 Rebholz C, Ziegele H, Leyland A et al. (1998) Structure, mechanical and tribological properties of Ti-B-N and Ti-Al-B-N multiphase thin films produced by electron-beam evaporation. J Vac Sci Technol A 16:2851–2857
6 Rao CNR, Raveau B (1998) Colossal magnetoresistance charge ordering and related properties of manganese oxides. World Scientific, Singapore
7 Tokura Y, Nagosa N (2000) Orbital physics in transition-metal oxides. Science 288:462–468
8 Hu CD (2002) Low-temperature resistivity of double-exchange interaction systems. Phys Rev B 66:132404
9 Olmos L, Martin CL, Bouvard D (2009) Sintering of mixtures of powders: experiments and modeling. Powder Technol 190:134–140
10 Afarani MS, Samimi A, Yekta EB (2013) Synthesis of alumina granules by high shear mixer granulator: processing and sintering. Powder Technol 237:32–40
11 Larsson EM, Millet J, Gustafsson S, Skoglundh M (2012) Real time indirect nanoplasmonic in situ spectroscopy of catalyst nanoparticles sintering. Catalysis 2:238–245
12 Ma J, Theingia M, Chen QM et al. (2013) Influence of synthesis methods and calcination temperature on electrical properties of $La_{1-x}Ca_xMnO_3$ (x=0.33 and 0.28) ceramics. Ceram Int 39:7839–7843
13 Phuc NX, Nguyen HaM, Manh DH et al. (2006) Perovskite nanoparticles: preparation by reactive milling and magnetic characteristics. Journal of Magnetism and Magnetic Materials 304:133–137
14 Manha DH, Phong PT, Thanh TD et al. (2010) Low-field magnetoresistance of $La_{0.7}Ca_{0.3}MnO_3$ perovskite synthesized by reactive milling method. J Alloys Comp 499:131–134
15 Mathur S, Shen H (2002) Structural and physical properties of $La_{2/3}Ca_{1/3}MnO_3$ prepared via a modified sol-gel method. J Sol-Gel Sci Techn 25:147–157
16 Vertruyen B, Fagnard J-F, Vanderbemden Ph et al. (2007) Electrical transport and magnetic properties of Mn_3O_4-$La_{0.7}Ca_{0.3}MnO_3$ ceramic composites prepared by a one-step spray-drying technique. J Eur Ceram Soc 27:3923–3926
17 Wang T, Fang XD, Dong WW et al. (2008) Mechanochemical effects on microstructure and transport properties of nanocrystalline $La_{0.8}Na_{0.2}MnO_3$ ceramics. J Alloys Comp 458:248–252
18 Matos I, Sério S, Lopes ME et al. (2011) Effect of the sintering temperature on the properties of nanocrystalline $Ca_{1-x}Sm_xMnO_3$ ($0 \leq x \leq 0.4$) powders. J Alloys Comp 509:9617–9626

19 Siwach PK, Prasad R, Gaur A et al. (2007) Microstructure-magnetotransport correlation in $La_{0.7}Ca_{0.3}MnO_3$. J Alloys comp 443:26–31
20 Fang ZZ, Wang H (2008) Densification and grain growth during sintering of nanosized particles. Int Mater Rev 53:326–352
21 Venkataiaha G, Krishnaa DC, Vithal M et al. (2005) Effect of sintering temperature on electrical transport properties of $La_{0.67}Ca_{0.33}MnO_3$. Phys B 357:370–379
22 Dhahri R, Halouni F (2004) Study of the effect of oxygen deficiencies on the $La_{1-x}(Sr,Ca)_xMnO_{3-\delta\square\delta}$ manganites properties. J Alloys comp 385:48–52
23 Sun JR, Rao GH, Zhang YZ (1998) Effects of inhomogeneous oxygen content in $(La,Gd)_{0.7}Ca_{0.3}MnO_{3+\delta}$ perovskites. Appl Phys Lett 72:3208
24 Venkataiah G, Prasad V, Venugopal Reddy P (2007) Influence of A-site cation mismatch on structural, magnetic and electrical properties of lanthanum manganites. J Alloys Comp 429:1–9
25 Markovich V, Fita I, Puzniak R et al. (2002) Magnetization and ac susceptibility studies of the magnetic phase separation in $La_{0.8}Ca_{0.2}MnO_3$ and $La_{0.78}Ca_{0.22}MnO_3$ single crystals. PhysRev B 66:094409